



Numerical Simulation of Flash Boiling Effect in a 3-Dimensional Chamber Using Computational Fluid Dynamic Techniques

S. Jafarmadar, A. Jahangirami*

Department of Mechanical Engineering, Faculty of Engineering, Urmia University, Iran

PAPER INFO

Paper history:

Received 01 March 2015

Received in revised form 31 December 2015

Accepted 05 January 2016

Keywords:

Flash Boiling
Numerical Simulation
Bubble Nucleation
Fuel Properties

ABSTRACT

Flash-boiling atomization is one of the most effective means of generating a fine and narrow-dispersed spray. Unless its complexity, its potential has not been fully realized. In this paper, a three dimensional chamber has been modeled with a straight fuel injector. Effect of flash-boiling has been investigated by computational fluid dynamics (CFD) techniques. A finite volume approach with the standard $k-\epsilon$ turbulence model has been used to carry out all the computations. The dimensions of studied vortex tubes are kept the same for all models. Finally, some results of the CFD models are validated by the available experimental data which show reasonable agreement, and other ones are compared qualitatively. It is confirmed that flash-boiling effectively accelerates the atomization and vaporization of fuel droplets.

doi: 10.5829/idosi.ije.2016.29.01a.12

1. INTRODUCTION

When a liquid, initially in a sub cooled state, is rapidly depressurized to a pressure sufficiently below the saturated vapor pressure, it can no longer exist in the liquid state, and a rapid boiling process called flash-boiling is initiated. Sudden evaporation of a portion of the fuel cools the rest of the liquid down and increases the spray volume.

In the case of high-pressure diesel injection, the phenomenon of flash-boiling can only be achieved if the fuel is sufficiently preheated before injection. In the case of gasoline injection, flash-boiling is much easier to obtain due to the lower boiling curve. Especially, if gasoline is injected to the intake manifold, where the static pressure can fall below the saturated vapor pressure of some hydrocarbon fuel components. Such a condition will result in unintended flash-boiling. This causes significant changes in the fuel spray distribution and the fuel-air mixing. Figure 1 shows the conventional and the flash-boiling fuel injection in a

pressure-enthalpy diagram. Subcooled liquid exists in the left of the liquid saturation line, and superheated vapor exists in the right of the vapor saturation line. By injection, the highly pressurized fuel leaves the nozzle's orifice and during this process, the liquid is strongly accelerated and the pressure decreases. In the case of conventional injection (line 1'- 2'), because the fuel temperature, and its enthalpy is too low it cannot cross the liquid saturation line during pressure decrease.

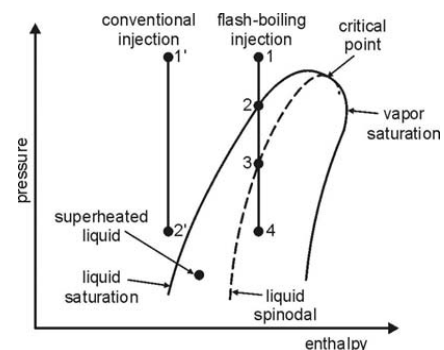


Figure 1. Comparison of conventional injection and flash-boiling injection [1]

*Corresponding Author's Email: ajahangirami@yahoo.com (A. Jahangirami)

Increasing fuel temperature results in a higher fuel enthalpy, so during injection the fuel undergoes a pressure reduction from point 1 to point 4 while passing through the nozzle orifice and flash-boiling occurs. After point 2 we have saturation condition and between this point and point 3, vapor bubbles are formed and begin to grow and beyond point 3 nucleation rates become large.

Numerous experimental studies of this injection type have been performed to examine the phenomenon in detail. Gerrish and Ayer [2] observed when diesel fuel was preheated prior to injection, spray cone angle increased. Kim et al. [3] confirmed that flash-boiling provides the benefits of the measurements of drop sizes, spray cone angle and penetration by performing flash-boiling studies with alcohol, in both an engine cylinder and a test chamber. Similar results were obtained by more fundamental experiments in atmospheric pressure chambers (e.g. [1-4]).

According to experimental investigations, depending on the degree of superheat; there are two main categories of flash-boiling sprays: external and internal flashing (e.g. [1, 5]). In the case of external flashing, evaporation and rapid bubble growth occurs outside the nozzle in the spray but in the case of internal flashing, rapid bubble growth occurs already inside the nozzle hole. The rapid bubble growth shatters the liquid jet and results in an increased spray cone angle and a reduced penetration, and bubble growth inside the nozzle hole results in an under-expanded compressible two-phase flow that expands immediately upon leaving the nozzle.

External flashing is difficult to obtain because a smooth nozzle entry geometry and/or low injection velocities must be used in order to avoid regions of locally low pressure inside the injection holes and to suppress internal flashing. Further on, careful matching of injection pressure and fuel temperature with combustion chamber pressure is necessary during the time of injection, because the degree of superheat and thus the change from the external to the internal flashing regime is very sensible to the chamber pressure. Hence, the relevant flashing regime is the internal flashing mode. However, internal flashing results in a reduction of effective cross-sectional area inside the injection hole and thus reduces the mass flow through the nozzle. At high degrees of superheat, the nozzle hole can become vapor-locked, and the mass flow reduces drastically [6]. In engine applications this has to be avoided in all cost.

Hence, the optimum degree of superheat is difficult to control, and this is one of the reasons why flash-boiling is not used today in series production engines. However, flash-boiling might become an important effect for future direct injection spark ignition (DISI) and homogeneous charge compression ignition (HCCI) engines because of the low gas pressures inside the combustion chamber during early injection.

An atomization model for superheated fuel sprays from pressure-swirl atomizers including the effect of flash-boiling has been recently developed by Zuo et al. [7]. It is assumed that under superheat conditions a hollow-cone spray sheet is still formed from the pressure-swirl atomizer, and the sheet flash-boiling is controlled by the rate of heat that can be conducted inside the sheet with an effective thermal conductivity. Hydrodynamic instability and cavitation and bubble growth finally break the sheet up to form drops. Models for the subsequent drop vaporization account for heat transfer under flash-boiling and sub-boiling conditions.

Further models considering the effect of flash-boiling on spray atomization, including detailed nucleation and bubble growth models, are published, for example, by Fujimoto et al. [8], Kawano [9] and Zeng and Lee [10]. The submodels for flash-boiling spray of multi component fuel which take account for fuel properties, vaporization process, bubble nucleation, growth and disruption in multi component fuel droplet were solved with Fluent and added to KIVA3V. The numerical data using these models were compared with experimental data. The flashing spray characteristics from numerical simulation qualitatively showed good agreement with the experimental results. In addition the effects of initial fuel temperature on the numerical results are investigated.

2. MATHEMATICAL FORMULATION

2. 1. Bubble Nucleation Bubble nucleation process is classified into two groups, that are the heterogeneous and homogeneous nucleations. In homogeneous nucleation, bubbles are created inside the liquid in the absence of any bubble nuclei. The process becomes predominant when the liquid pressure is greatly reduced corresponding to a tensile force opposed to the molecular force of the liquid. However, it is not necessary to consider this process because the decompression in the numerical simulation is quite weaker than the tensile force. The heterogeneous nucleation occurs when gas and solid phases appear at an interface or a boundary rather than in the liquid. In this process, an activated cluster grows to critical size and becomes a nucleus in the presence of crevices on the solid surface, fine solid particles, mixed gas or dissolved gas in the liquid. In connection with the nucleation from the solid surface, Sato et al. [11] reported that the spray characteristic was not affected by bubble nucleation in nozzle orifice, if the ratio of orifice length to orifice diameter (l/d) was less than 0.7. l/d of the injector orifice used in this study is less than 0.7 ($l/d=0.5$). In addition, used organic liquids well wet the solid surface compared with water [12]. Therefore, it implies that the nucleation from the solid surface is

negligible in this study. It is difficult to treat quantitatively the nucleation process due to fine dust or minute solid particles inside the liquid. Furthermore, fuel is well filtered for the experiments. Therefore, the nucleation due to dust is neglected in this study. Accordingly, only heterogeneous nucleation owing to dissolved gas as air is considered in this study. Regarding this process, it has been experimentally confirmed that the number density of bubble nuclei exponentially increased by the increase in the superheating degree for the superheated flash-boiling process [1, 12]. In general, it is assumed that the number density of bubble nuclei in the liquid N is constant throughout the fuel injection process in the above equation [13]. However, dissolved gas or air in the liquid is consumed by bubble nucleation. Therefore, it is supposed that N decreases as the time elapses in the nozzle orifice and droplets. It is reported that the number of bubble nuclei obtained by numerical simulation applied in this assumption agrees with the experimental data [14]. The number density N of bubble nuclei is approximately expressed by the following equation:

$$N = 1.11 \times 10^{12} \cdot \exp\left(\frac{-5.28}{\Delta\theta}\right) \{10^{-4.34 \exp(-5t)}\} \quad (1)$$

where $\Delta\theta$ is the superheating degree of the liquid.

2. 2. Bubble Growth

The bubble is assumed to grow spherically in nozzle orifice and droplets and the Rayleigh-Ples set equation [15] describes the growth process of the cavitation bubble. The growth rate of the cavitation bubble is controlled by hydrodynamics forces as follows:

$$R\ddot{R} + \frac{3}{2}\dot{R}^2 = \frac{1}{\rho}(P_w - P_r) \quad (2)$$

where ρ is the liquid density and P_r is the pressure around bubble. The fluid pressure at bubble surface, P_w , is defined by the following equation [16]:

$$P_w = P_v + (P_{r0} + \frac{2\sigma}{R_0}) \left(\frac{R_0}{R}\right)^{3n} - \frac{2\sigma}{R} - \frac{4\mu\dot{R}}{R} - \frac{4k\dot{R}}{R^2} \quad (3)$$

where P_v is the saturation pressure of fuel, P_r is the initial fluid pressure around bubble, R_0 is the initial bubble radius, μ_l is liquid viscosity and κ is the surface viscosity coefficient proposed by Scriven [17]. However, κ used in this equation has the value presented in the previous paper ($\kappa=8.0 \times 10^{-6}$ [N·s/m]) [16].

2. 3. Bubble Disruption

There is a limit in the growth of bubbles inside droplet. This limit is determined by the diameter of the droplet, surface tension and liquid viscosity, then number density of bubble nuclei and growth rate.

The limit of bubble growth rate inside droplet is

provided with the void fraction, ε , defined by the volume ratio between the vapor and liquid phases as the following equation:

$$\varepsilon = \frac{V_{bubble}}{V_{bubble} + V_{liquid}} \quad (4)$$

where, V_{bubble} is volume of bubbles and V_{liquid} is volume of liquid. Suma et al. [18] mentioned that breakup of fuel jet occurred at $\varepsilon=0.51$ to 0.53 [18]. In this study, it is assumed that the droplet is broken up when the calculated void fraction reaches to 0.55 , considering the apparent increase in the liquid viscosity of two-phase flow. Then, it is supposed that the droplet is broken up into small droplets twice as many as the number of bubbles, as illustrated in Figure 2.

As a consequence, both the number and diameter of droplets after breakup caused by bubble disruption can be calculated. The momentum of the parent droplet is uniformly distributed among the child droplets.

2. 4. Conservation Equation's and Turbulence Formulation

The governing equations are arranged by the conservation of mass, momentum and energy equations, which are given by:

$$\frac{\partial}{\partial t}(\rho) + \frac{\partial}{\partial x_j}(\rho \tilde{u}_j) = 0 \quad (5)$$

$$\frac{\partial}{\partial t}(\rho u_i) + \frac{\partial}{\partial x_j}(\rho \tilde{u}_j u_i - \tau_{ij}) = -\frac{\partial p}{\partial x_i} \quad (6)$$

$$\frac{\partial}{\partial x_j} \left[u_i \rho \left(h + \frac{1}{2} \tilde{u}_j \tilde{u}_j \right) \right] = \quad (7)$$

$$\frac{\partial}{\partial x_j} \left[k_{eff} \frac{\partial T}{\partial x_j} + u_i (\tau_{ij})_{eff} \right] \& \quad k_{eff} = K + \frac{c_p \mu_t}{Pr_t}$$

Since we assumed the working gas is an ideal gas, then the compressibility effect must be imposed so that:

$$p = \rho RT \quad (8)$$

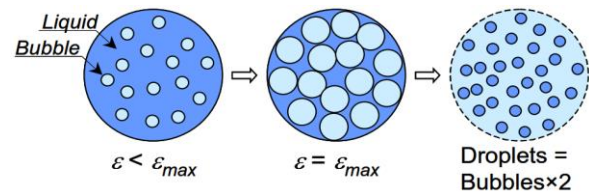


Figure 2. Breakup caused by bubble disruption

The turbulence kinetic energy (k) and the rate of dissipation (ε) are obtained from the following equations:

$$\begin{aligned} \frac{\partial}{\partial t}(\rho k) + \frac{\partial}{\partial x_i}(\rho k u_i) = \\ \frac{\partial}{\partial x_j} \left[\left(\mu + \frac{\mu_t}{\sigma_k} \right) \frac{\partial k}{\partial x_j} \right] + G_k + G_b - \rho \varepsilon - Y_M \end{aligned} \quad (9)$$

$$\begin{aligned} \frac{\partial}{\partial t}(\rho\varepsilon) + \frac{\partial}{\partial x_i}(\rho\varepsilon u_i) = \\ \frac{\partial}{\partial x_j} \left[\left(\mu + \frac{\mu_t}{\sigma_k} \right) \frac{\partial \varepsilon}{\partial x_j} \right] + C_{1\varepsilon} \frac{\varepsilon}{k} (G_k + C_{3\varepsilon} G_b) - \\ C_{2\varepsilon} \rho \frac{\varepsilon^2}{k} \end{aligned} \quad (10)$$

In these equations, G_k , G_b , and Y_M represent the generation of turbulence kinetic energy due to the mean velocity gradients, the generation of turbulence kinetic energy due to buoyancy and the contribution of the fluctuating dilatation in compressible turbulence to the overall dissipation rate, respectively. $C_{1\varepsilon}$ and $C_{2\varepsilon}$ are constants. σ_k and σ_ε are the turbulent Prandtl numbers for k and ε also. The turbulent (or eddy) viscosity, μ_t , is computed as follows:

$$\mu_t = \rho C_\mu \frac{k^2}{\varepsilon} \quad (11)$$

where, C_μ is a constant. The model constants $C_{1\varepsilon}$, $C_{2\varepsilon}$, C_μ , σ_k and σ_ε have the following default values: $C_{1\varepsilon} = 1.44$, $C_{2\varepsilon} = 1.92$, $C_\mu = 0.09$, $\sigma_k = 1.0$, $\sigma_\varepsilon = 1.3$.

Finite volume method with a 3D structured mesh is applied to the mentioned governing equations. Table 1 summarizes the conditions for the numerical simulation. As a fuel, the mixture of 75 mol% n-pentane (C_5H_{12}) and 25 mol% n-tridecane ($C_{13}H_{28}$) was used. Initial ambient temperature and pressure were 440 K and 0.1MPa, respectively. Initial fuel temperature T_f was varied to 320, 380 and 440 K for the control of flash boiling process. Injection velocity of 10316.4 cm/s was calculated from Bernoulli's equation in order to correspond to 15 MPa of injection pressure. Second order upwind scheme is utilized to discretize convective terms, and SIMPLE algorithm is used to solve the momentum and energy equations simultaneously.

2. 5. Bubble Dynamics Equation: Rayleigh-Plesset Equation

Consider a spherical bubble of radius, $R(t)$ (where t is time), in an infinite domain of liquid whose temperature and pressure far from the bubble are T and $p(t)$, respectively. The temperature, T , is assumed to be a simple constant since temperature gradients were eliminated, a priori and uniform heating of the liquid due to internal heat sources or radiation will not be considered. On the other hand, the pressure, $p(t)$, is assumed to be a known (and perhaps controlled) input which regulates the growth or collapse of the bubble.

Though compressibility of the liquid can be important in the context of bubble collapse, it will, for the present, be assumed that the liquid density, ρ_L , is a constant. Furthermore, the dynamic viscosity, ν_L , is assumed constant and uniform. It will also be assumed that the contents of the bubble are homogeneous and that the temperature, $T_B(t)$, and pressure, $p_B(t)$, within the bubble are always uniform. These assumptions may not be justified in circumstances that will be identified

as the analysis proceeds.

The radius of the bubble, $R(t)$, will be one of the primary results of the analysis. As indicated in Figure 3, radial position within the liquid will be denoted by the distance, r , from the center of the bubble; the pressure, $p(r,t)$, radial outward velocity, $u(r,t)$, and temperature, $T(r,t)$, within the liquid will be so designated. Conservation of mass requires that

$$u(r,t) = \frac{F(t)}{r^2} \quad (12)$$

where $F(t)$ is related to $R(t)$ by a kinematic boundary condition at the bubble surface. In the idealized case of zero mass transport across this interface, it is clear that $u(R,t) = dR/dt$ and hence:

$$F(t) = R^2 \frac{dR}{dt} \quad (13)$$

TABLE 1. Numerical conditions

Fuel	$C_5H_{12} / C_{13}H_{28}$ 0.75 : 0.25 (mol %)
Ambient gas	N_2
Ambient pressure	0.1 MPa
Ambient temperature	440 K
Hole diameter	0.2 mm
Injection velocity	10316.4 cm/s
Initial fuel temperature	320, 380, 440 K
Initial time step	1.0 ms
Number of parcel	1000

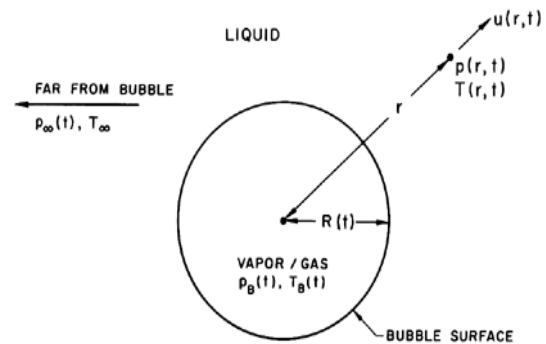


Figure 3. Schematic of a spherical bubble in an infinite liquid.

But this is often a good approximation even when evaporation or condensation is occurring at the interface. To demonstrate this, consider a vapor bubble. The volume rate of production of vapor must be equal to the rate of increase of size of the bubble, $4\pi R^2 dR/dt$, and therefore the mass rate of evaporation must be $\rho_V(T_B) 4\pi R^2 dR/dt$ where $\rho_V(T_B)$ is the saturated vapor density at the bubble temperature, T_B . This, in turn, must equal the mass flow of liquid inward relative to the interface, and hence the inward velocity of liquid relative to the interface is given by $\rho_V(T_B)(dR/dt) / \rho_L$.

Therefore:

$$u(R, t) = \frac{dR}{dt} - \frac{\rho v(T_B)}{\rho_L} \frac{dR}{dt} = \left[1 - \frac{\rho v(T_B)}{\rho_L} \right] \frac{dR}{dt} \tag{14}$$

and

$$F(t) = \left[1 - \frac{\rho v(T_B)}{\rho_L} \right] R^2 \frac{dR}{dt} \tag{15}$$

In many practical cases $\rho v(T_B) / \rho_L$ and therefore the approximate form of Equation (13) may be adequate. For clarity we will continue with the approximate form given in Equation (13).

Assuming a Newtonian liquid, the Navier-Stokes equation for motion in the r direction yields after substituting for u from $u=F(t)/r^2$:

$$-\frac{1}{\rho_L} \frac{\partial p}{\partial r} = \frac{\partial u}{\partial t} + u \frac{\partial u}{\partial r} - \nu_L \left[\frac{1}{r^2} \frac{\partial}{\partial r} (r^2 \frac{\partial u}{\partial r}) - \frac{2u}{r^2} \right] \tag{16}$$

$$-\frac{1}{\rho_L} \frac{\partial p}{\partial r} = \frac{1}{r^2} \frac{dF}{dt} - 2 \frac{F^2}{r^5} \tag{17}$$

Note that the viscous terms vanish; indeed, the only viscous contribution to the Rayleigh-Plesset Equation comes from the dynamic boundary condition at the bubble surface. Equation (16) can be integrated to give:

$$\frac{p - p_\infty}{\rho_L} = \frac{1}{r} \frac{dF}{dt} - \frac{1}{2} \frac{F^2}{r^4} \tag{18}$$

Finally Rayleigh-Plesset equation for bubble dynamics generalized as bellow:

$$\frac{p_B(t) - p_\infty(t)}{\rho_L} = R \frac{d^2R}{dt^2} + \frac{3}{2} \left(\frac{dR}{dt} \right)^2 + \frac{4\nu_L dR}{R dt} + \frac{2S}{\rho_L R} \tag{19}$$

It was first derived and used by Rayleigh (1917). Plesset (1949) first applied the equation to the problem of traveling cavitation bubbles.

3. PHYSICAL MODELING

Figure 4 shows the computation algrid for this computation. This gridis assumed a circular cylinder shaped constant volume vessel which is 100 mm in height and 60 mm in diameter. Nozzle modeled as a hole on top of the cylinder with 0.2 mm in diameter. The geometry of the model and present created CFD model is identical to the experimental data's of Kawano et al. [19]. In this numerical research, all geometrical properties of the Kawano et al. [19] model are kept constant and effect of flash-boiling was investigated under different kinds of fuels and temperatures. The 3-D CFD model with refinement in mesh along with boundary regions is shown in Figure 4.

Boundary conditions for the models are determined based on the experimental measurements by Kawano et al. [19]. The inlet is modeled as a velocity inlet. Mechanism of injection can be changed with its inlet parameters. In addition, a no-slip velocity boundary

condition is enforced on all of the walls of vortex tube, and simultaneously they are assumed to be adiabatic.

Figure 5 shows the effect of initial fuel temperature variations on pressure-temperature diagram for the mixed fuel. In this case, it is peculiar that “two-phase region” which has both liquid and vapor phases appears on this diagram. In this diagram, upper and lower borderlines of the two-phase region correspond to the saturation liquid and vapor lines, respectively. Furthermore, it is easy to obtain the flash-boiling effect using a mixture, because the critical point of the mixture is shifted to higher pressure side, compared to each single component fuel. The conditions of the fuel which is injected into the combustion chamber at each initial fuel temperature established in this study are represented in this figure as the bold line. The state at $T_f=320$ K is just on the saturation liquid line of the two-phase region. In case of $T_f=380$ and 440 K, the mixed fuel directly passes through the two-phase region crossing saturation liquid line during decompression process and decompression degree (= saturation pressure – ambient pressure) is enhanced with increases in T_f . Especially, in case of $T_f=440$ K, mixed fuel can be directly reached to ambient condition by only decompression process.



Figure 4. Three-dimensional CFD model of chamber

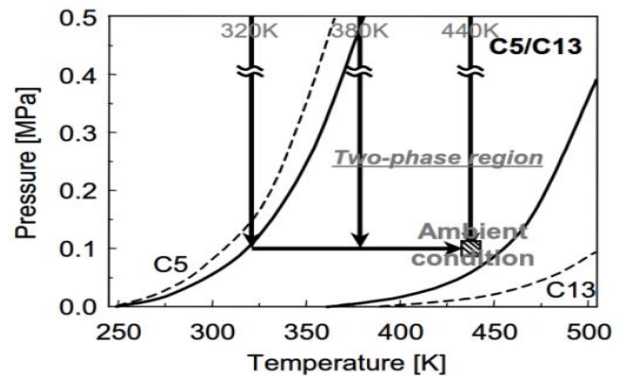


Figure 5. Initial fuel temperature variations

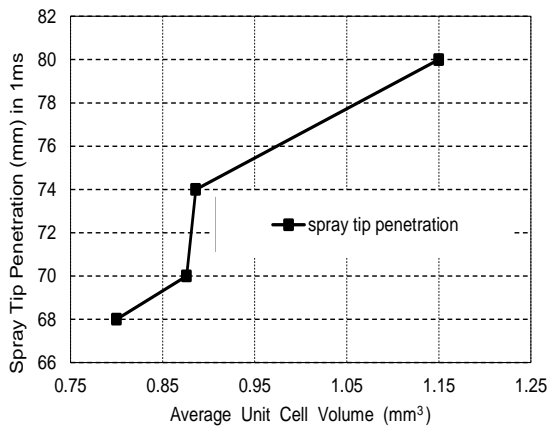


Figure 6. Grid size independence study at different average unit cell volumes.

5. RESULTS AND DISCUSSIONS

5.1. Grid Independence Study The 3-D CFD analysis has been carried out for different average unit cell volumes in chamber as a computational domain. This is because of removing probable errors arising due to grid coarseness. Hence, first the grid independence study has been accomplished for inlet temperature of 320 K. The spray tip penetration in 1ms after injection as the key parameter is shown in Figure 6 for different unit cell volumes. Not much significant advantage can be seen by reducing the unit cell volume size below 0.8 mm³; which corresponds to 371100 cells. The same type of unit cell volume of grids is used to study the introduced chamber.

5.2. Droplet and Vapor Distributions Figure 7 shows the droplet and vapor distributions for each initial fuel temperature at time from start of injection $t_{inj}=1.0$ ms. In this figure, shadow graph images which are obtained by the previous experiment using constant

volume vessel [19] are added. In case of $T_f=320$ K at which flash-boiling does not occur, n-tridecane does not almost vaporize. The state of the fuel lies on saturation liquid line as can be seen in Figure 4. Even then, n-tridecane cannot evaporate, because the ambient temperature is comparatively low and it is not easy to heat up liquid droplets.

Both n-pentane and n-tridecane well vaporize at $T_f=380$ K at which flashing occurs. High vapor concentration region of n-pentane is located at upstream of fuel spray. On the other hand, the fuel spray also has high vapor concentration region of n-tridecane at the downstream. It is reported that vaporization process of multicomponent fuel depends on batch-distillation from the result of spray experiments [20, 21].

The batch-distillation of multicomponent fuel spray is maintained in spite of flashing or non-flashing. The trend in the batch-distillation at $T_f=440$ K becomes more remarkable and both n-pentane and n-tridecane actively vaporize because of violent flashing due to large decompression degree. The spray widths at $T_f=380$ and 440 K obtained from gas phase in numerical results seem to be much larger than the experimental one. However, it was observed that, in case of $T_f=380$ and 440 K, lean mixture disperses to radial direction near nozzle orifice [19]. This dispersion cannot be clearly observed in Figure 5. It can be thought that this phenomenon is occurred by violent flashing, since it is not possible to observe that at $T_f=320$ K. Therefore, the drastic increase in spray width due to flashing can be predicted using this model.

Velocity vectors colored by their magnitude is shown in Figure 8 to consider exact flow pattern in injection process in case of $T_f=320$ K and $T_f=380$ K.

The spray widths at $T_f=380$ and 440 K obtained from gas phase in numerical results seem to be much larger than the experimental one. However, it was observed that, in case of $T_f=380$ and 440 K, lean mixture disperses to radial direction near nozzle orifice [19].

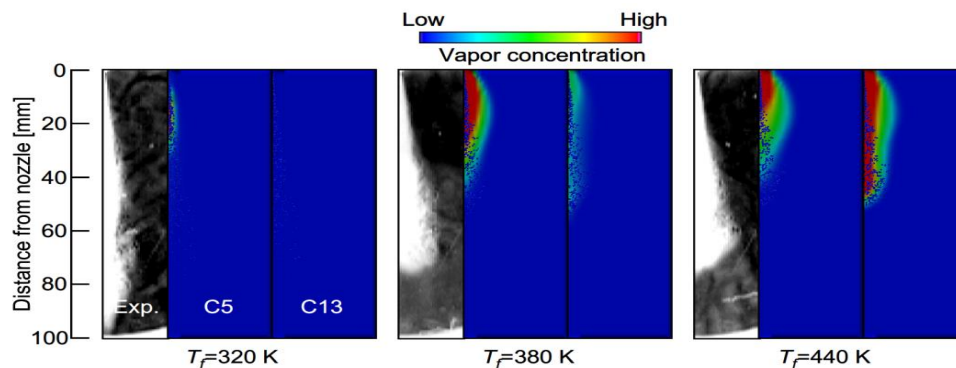


Figure 7. Droplet and vapor distributions for each initial fuel temperature at time from start of injection $t_{inj}=1.0$ ms.

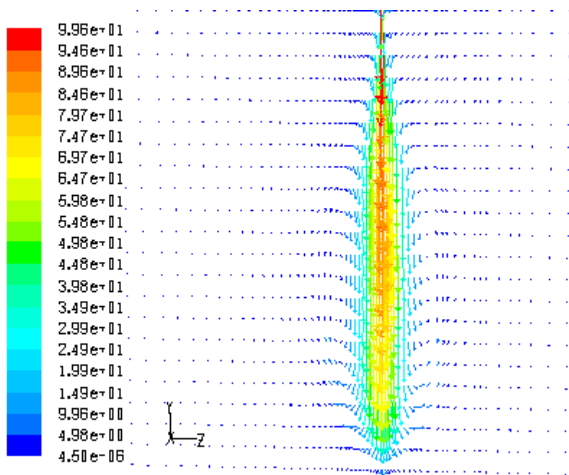


Figure 8 a. Velocity vectors in case of $T_f=320$ K

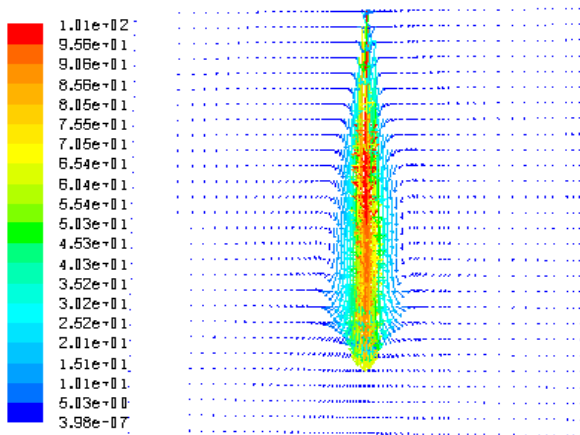


Figure 8 b. Velocity vectors in case of $T_f=380$ K

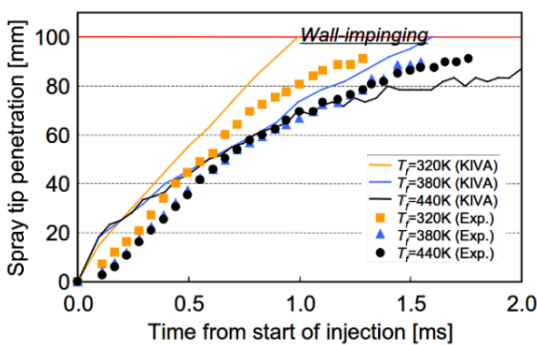


Figure 9. Fuel penetration

This dispersion cannot be clearly observed in Figure 5. It can be thought that this phenomenon occurs by violent flashing, since it is not possible to observe that at $T_f=320$ K. Therefore, the drastic

increase in spray width due to flashing can be predicted using this model. Velocity vectors colored by their magnitude is shown in Figure 8 to consider exact flow pattern in injection process in case of $T_f=320$ K and $T_f=380$ K.

5. 3. Fuel Penetration

Figure 9 indicates the experimental and numerical results of fuel penetration. In case of $T_f=320$ K, fuel linearly penetrates up to impingement on the wall. Nevertheless, numerical fuel penetrations of $T_f=320$ K are slightly longer than the experimental one. In this model, the parameters in droplet break up model (TAB model) are optimized to approximate the under estimated droplet size derived from the original TAB model to real droplet size of diesel spray [22]. Therefore, it is estimated that this improvement produces large droplets and the fuel penetration is overestimated, especially under low ambient pressure. On the other hand, numerical fuel penetrations of $T_f=380$ and 440 K are shorter than that at $T_f=320$ K due to flash-boiling as can be seen from Figure 6. The penetration trace at $T_f=440$ K is similar to that at $T_f=380$ K in spite of the different decompression degree, and this trend can be seen from the experimental data. It is estimated that penetration at $T_f=440$ K is made longer by droplet cooling effect of much latent heat of vaporization. Therefore, this model can correctly predict the short fuel penetration of flashing spray.

6. CONCLUSION

From the numerical investigation of the effect of flash-boiling on spray characteristics of multicomponent fuel, the following conclusions are obtained.

- Flash-boiling processes (bubble nucleation, growth and disruption) in multicomponent fuel droplets and nozzle orifice are modeled.
- In case of $T_f=380$ K, batch-distillation which is peculiar to multicomponent fuel is observed, and especially this trend becomes more remarkable at $T_f=440$ K.
- The fuel linearly penetrates up to impingement on the wall at $T_f=320$ K. The numerical fuel penetrations of $T_f=380$ and 440 K are shorter than that at $T_f=320$ K due to flash-boiling. This trend agrees with experimental data.
- In case of $T_f=320$ K, both n-pentane and n-tridecane do not vaporize. On the contrary, both components completely vaporize after $t_{inj}=1.0$ ms at $T_f=440$ K.
- The droplet size distribution at $T_f=380$ and 440 K

is drastically shifted to small droplet side due to flashing, compared with that at $T_f=320$ K.

7. REFERENCES

- Oza, R.D. and Sinnamon, J.F., An experimental and analytical study of flash-boiling fuel injection., SAE Technical Paper. (1983)
- Gerrish, H.C. and Ayer, B.E., "Influence of fuel-oil temperature on the combustion in a prechamber compression-ignition engine", *NACA Technical Note* (1936), 565-577
- Kim, Y., Iwai, N., Suto, H. and Tsuruga, T., Improvement of alcohol engine performance by flash boiling injection. *JSAE Review*, No 2, (1980) 81–86.
- Wu, K., Steinberger, R. and Bracco, F., "On the mechanism of breakup of highly superheated liquid jets", *Paper No. CSS/CI*, (1981), 81-17.
- Park, B.S. and Lee, S.Y., "An experimental investigation of the flash atomization mechanism", *Atomization and Sprays*, Vol. 4, No. 2, (1994) 102-134.
- Reitz, R.D., "A photographic study of flash-boiling atomization", *Aerosol Science and Technology*, Vol. 12, No. 3, (1990), 561-569.
- Zuo, B., Gomes, A. and Rutland, C., "Modelling superheated fuel sprays and vaporization", *International Journal of Engine Research*, Vol. 1, No. 4, (2000), 321-336.
- Fujimoto, H., Mishikori, T., Tsukamoto, T. and Senda, J., "Modeling of atomization and vaporization process in flash boiling spray", *ICLASS-94, Paper VI-13.*, (1994) 36-49.
- Kawano, D., Ishii, H., Suzuki, H., Goto, Y., Odaka, M. and Senda, J., "Numerical study on flash-boiling spray of multicomponent fuel", *Heat Transfer—Asian Research*, Vol. 35, No. 5, (2006), 369-385.
- Zeng, Y. and Lee, C.-F.F., "An atomization model for flash boiling sprays", *Combustion Science and Technology*, Vol. 169, No. 1, (2001), 45-67.
- Sato, K., Lee, C. and Nagai, N., "A study on atomization process of superheated liquid", *Transactions of JSME (B)*, Vol. 50, No. 455, (1984), 1743-1752.
- Nakamura, K. and Someya, T., "Investigation on the tensile strength of real liquids", *Transactions of JSME (B)*, Vol. 46, No. 405, (1987), 910-917.
- Van Stralen, S. and Cole, R., "Boiling phenomena: Physicochemical and engineering fundamentals and applications, *Hemisphere Pub.(Washington)*, Vol. 2, (1979). 104-142 .
- Adachi, M., McDonell, V.G., Tanaka, D., Senda, J. and Fujimoto, H., Characterization of fuel vapor concentration inside a flash boiling spray., *SAE Technical Paper* (1997)
- Plesset, M. S., Cavitation in Real Liquids, Amer. Elsevier Pub. (New York), (1964) 1-14.
- Ida, T. and Sugiyama, T., "Motion of air bubbles in mineral oils subject to sudden change in chamber pressure (1st report, experimental analysis for single bubbles)(in japanese)", *Transactions of JSME 45–399*, (1979), 1650-1657.
- Scriven, L., "Dynamics of a fluid interface equation of motion for newtonian surface fluids", *Chemical Engineering Science*, Vol. 12, No. 2, (1960), 98-108.
- Suma, S. and Koizumi, M., "Internal boiling atomization by rapid pressure reduction of liquids", *Transactions of the Japanese Society of Mechanical Engineers*, Vol. 43, No. 376, (1977), 4608-4617.
- Kawano, D., Azechi, N., Senda, J. and Fujimoto, H., "Spray Characteristics of Multicomponent Fuel", The 10th International Symposium on Flow Visualization, F0219, (2002) 65-72.
- Akihama, K., Fujikawa, T. and Hattori, Y., "Simultaneous laser-induced fluorescence measurements of in-cylinder fuel behavior of different boiling point components", in Proc. 15th Internal Combustion Engine Symposium (International), Seoul. (1999), 577-582.
- Styron, J.P., Kelly-Zion, P., Lee, C.-F., Peters, J., White, R.A. and Lucht, R., Multicomponent liquid and vapor fuel distribution measurements in the cylinder of a port-injected, spark-ignition engine., *SAE Technical Paper*. (2000), 87-96
- Kawano, D., Senda, J., Wada, Y., Fujimoto, H., Goto, Y., Odaka, M., Ishii, H. and Suzuki, H., *Numerical Simulation of Multicomponent Fuel Spray.*, SAE Technical Paper, (2003).

Numerical Simulation of Flash Boiling Effect in a 3-Dimensional Chamber Using Computational Fluid Dynamic Techniques

S. Jafarmadar, A. Jahangirami

Department of Mechanical Engineering, Faculty of Engineering, Urmia University, Iran

PAPER INFO

چکیده

Paper history:

Received 01 March 2015

Received in revised form 31 December 2015

Accepted 05 January 2016

Keywords:

Flash Boiling

Numerical Simulation

Bubble Nucleation

Fuel Properties

اتمی‌زاسیون به روش جوشش سریع یکی از فرایندهای مهم در تولید اسپری می باشد برخلاف پیچیدگی آن توانایی این فرایند تاکنون به خوبی کشف نشده است. در این بررسی، یک محفظه ۳ بعدی با یک نازل سوخت مستقیم مدلسازی گردیده است. تاثیر پدیده جوشش سریع با استفاده از روش دینامیک سیالات محاسباتی مطالعه شده و یک روش حجم محدود با بکارگیری مدل استاندارد توربولانس $k-\epsilon$ برای حل معادلات بکارگیری شده است. ابعاد مدل‌های ساخته شده برای تمامی حالات یکسان در نظر گرفته شده است. در نهایت نتایج کار عددی حاصل با نتایج کارهای تجربی موجود مقایسه و نتیجه حاصل رضایت بخش می باشد. بررسی حاصل نشان دهنده این واقعیت می باشد که پدیده جوشش سریع شدیداً اتمی‌زاسیون و تبخیر قطرات سوخت را شتاب می دهد.

doi: 10.5829/idosi.ije.2016.29.01a.12
